ORIGINAL PAPER

Using PFC[2D] to simulate the shear behaviour of joints in hard crystalline rock

Francisco Ríos-Bayona[1] · Fredrik Johansson[1] · Diego Mas-Ivars[1,2] · Abel Sánchez-Juncal[3,4] · Axel Bolin[5]

Abstract

Significant uncertainties remain regarding the assessment of the peak shear strength of rock joints. In recent years, Particle Flow Code (PFC) has been used to simulate shear tests of rock joints. Although previous studies showed PFC's capability to simulate rock joint shear behaviour, it is uncertain how different parameters in PFC should be combined to realistically capture roughness and strength of asperities in contact of actual rock joints. Under low normal stresses, the shear behaviour of well-mated hard crystalline joints is governed by the interaction between asperities of some tenths of a millimetre. This paper investigates the capability of PFC[2D] to realistically simulate the peak shear strength of hard crystalline rock joints under different constant normal stress magnitudes. The simulated two-dimensional profiles were selected from the digitised joint surface obtained with optical scanning measurements. To realistically capture surface roughness and asperity strength in PFC[2D], different values of joint segment length, particle resolution per segment, and bond strength between particles were studied and calibrated while taking into account the laboratory observations. The results of the numerical simulations in the PFC[2D] environment show that the simulated peak shear strength using the profile containing the steepest asperity is in good agreement with that measured in the laboratory. The joint profile needs to be represented by both a magnitude of segment length that captures the grain size, and at least two particles per segment. The bond strength calibration needs to account for both asperity size and the number of particles in contact during shearing.

Keywords Numerical direct shear test · PFC[2D] · Hard rock · Rock joints · Peak shear strength

✉ Francisco Ríos-Bayona
   frrb@kth.se

   Fredrik Johansson
   fredrik.johansson@byv.kth.se

   Diego Mas-Ivars
   diego.masivars@skb.se

   Abel Sánchez-Juncal
   abelsanchezjuncal@gmail.com

   Axel Bolin
   axel.bolin@trafikverket.se

1 Division of Soil and Rock Mechanics, Department of Civil and Architectural Engineering, KTH Royal Institute of Technology, Brinellvägen 23, Stockholm 100 44, Sweden

2 SKB Swedish Nuclear Fuel and Waste Management Co, Solna, Sweden

3 A&P Consultants, Edmonton, Canada

4 Previously at Itasca Consultants AB, Stockholm, Sweden

5 Swedish Transport Administration, Stockholm, Sweden

Introduction

In rock mechanics, it is necessary to be able to assess the shear strength of rock joints in order to solve different rock mechanical problems; this includes, for example, slope stability, block and arching stability in tunnels and the sliding stability of dams. In recent decades, various attempts have been made to develop empirical and analytical criteria to increase the understanding of the peak shear strength of rock joints (e.g., Patton 1966; Ladanyi and Archambault 1969; Barton and Choubey 1977; Grasselli and Egger 2003; Johansson and Stille 2014; Yang et al. 2016; Casagrande et al. 2018; Ban et al. 2020; Ríos-Bayona et al. 2021, 2022).

However, despite the proposed criteria, there is still uncertainty in the estimation of the shear strength of rock joints. In recent years, the emergence of advanced software has made it possible to use numerical modelling as a tool for studying the mechanical behaviour of jointed rock masses (Potyondy and Cundall 2004; Mas Ivars et al. 2011; Sinha and Walton 2020; Castro-Filgueira et al. 2020; Tang et al.

2020). Furthermore, various studies have used the software PFC developed by Itasca (2018) to numerically investigate the shear behaviour of rock joints. For instance, Cundall (2000), Park and Song (2009) and Asadi et al. (2012) used PFC to study the shear behaviour of rough rock joints with triangular, sinusoidal, and standard *JRC* profiles applying the bond removal method between particles on each side of the joint profile. In the bond removal method, the contact between particles that are within a specific distance on both sides of the joint profile is left unbounded. Although these studies demonstrated the capability of PFC to capture the principal shear behaviour of rough rock joints, the bond removal method suffered from unrealistic high micro-roughness due to the curvature of the particles used (Bahaaddini et al. 2013).

In an attempt to solve the shortcomings of the bond removal method and better reproduce the shear behaviour of rock joints numerically, the smooth-joint contact model (SJCM) proposed by Cundall in 2005 (Mas Ivars et al. 2008) was later used and applied to the particles in contact on each side of the joint profile (Bahaaddini et al. 2013; Lambert and Coll 2014; Lazzari et al. 2014). In the SJCM, particles on different sides of the joint profile are allowed to pass through each other instead of moving around one another. Applying the properties of the SJCM, Lambert and Coll (2014) used PFC^{3D} to numerically study the shear behaviour of an actual granite rock joint whose surface roughness had been previously measured with optical scanning by Grasselli et al. (2002). However, the results from the numerical shear tests performed by Lambert and Coll (2014) were not compared to the actual shear test conducted in the laboratory. Additionally, the three-dimensional surface roughness utilised in the numerical calculations had a resolution of 1.4 by 1.4 mm. This resolution is not sufficient to accurately capture surface roughness at the grain scale (Grasselli 2001; Grasselli and Egger 2003; Tatone and Grasselli 2009). In a similar attempt, Lazzari et al. (2014) used the optical scanning measurement of the surface roughness of an actual rock joint to numerically study its shear behaviour in PFC^{2D}. They compared the results of the numerical simulation with the actual laboratory direct shear test. However, the comparison made between the numerical and the actual shear tests was not a clear success since interlocking of single particles presented a major problem in their shear test environment. According to Lazzari et al. (2014), it could happen that certain particles, initially located above the joint profile, lied below the joint profile after the application of the normal stress (σ_n) used in the numerical simulations. Based on their results, interlocking due to these single particles occurred after a shear displacement of approximately one particle diameter, when the particles changing side were about to create new contacts with neighbour particles. This is the same phenomenon as the one observed by Bahaaddini et al. (2013). Furthermore, the two-dimensional profile that

they used in the numerical simulation was based on a simplification of the optical scanning of the actual surface roughness. To overcome the particle interlocking problem, Bahaaddini et al. (2013) proposed the shear box genesis (SBG) approach. This methodology includes the detection of particles situated in the upper and lower parts of the numerical rock specimen and allows for the generation of new SJCM along the joint plane during the numerical shear test. Bahaaddini et al. (2013) used PFC^{2D} and applied the SBG approach in order to numerically study the shear behaviour of saw-tooth triangular joints and standard *JRC* profiles on Hawkesbury sandstone. Most recently, similar approaches have been used to numerically study the scale effect of rock joints (Bahaaddini et al. 2014), improve the application of the SJCM (Mehranpour and Kulatilake 2017), study the shear behaviour of rock-concrete surfaces in dam foundations (Gutiérrez-Ch et al. 2018), and study the mechanical behaviour of synthetic rock joint profiles generated with self-affine fractal theory (Ríos-Bayona et al. 2018).

The above review shows that a methodology in PFC to realistically account for the surface roughness of actual rock joints measured with optical scanning and successfully compare numerically simulated and actual laboratory shear tests is still lacking. The only exception is Li et al. (2020), who used PFC^{2D} to compare a numerically simulated direct shear test with an actual laboratory test conducted on a perfectly mated rock joint sample of granite tested under a constant σ_n of 30 MPa. The two-dimensional joint profile tested by Li et al. (2020) had been selected through the steepest asperity. Although their results showed good agreement between the numerical and actual shear tests, it is uncertain if they are applicable for modelling the shear behaviour of hard crystalline rocks under lower σ_n to joint compressive strength ratios, which are typical in civil engineering applications. Furthermore, the governing asperities in contact under low σ_n, especially in well-mated joints in hard crystalline rocks, are on the order of some tenths of a millimetre (Johansson 2016). Therefore, modelling the strength and size of the active asperities in contact becomes more relevant in PFC to capture the actual shear behaviour of rock joints in these types of rocks. However, it is not clear how the resolution of the optical scanning measurements of hard crystalline rock joints should be combined with the calibration of the different parameters available in PFC to realistically account for their surface roughness and the strength of the asperities in contact in the numerical simulations.

Taking up this challenge, this paper investigates the capability of PFC^{2D} to realistically simulate the peak shear strength of hard crystalline rock joints under different applied constant σ_n magnitudes. To achieve this aim, this paper presents a methodology in PFC^{2D} that uses the surface measurements of a rock joint obtained with optical scanning

at a resolution that captures grain scale detail. Furthermore, to realistically account for the surface roughness and the strength of the active asperities during the shearing process in PFC^{2D}, the scanning measurements are combined with the calibration of joint segment length, particle resolution per segment, and bond strength between particles.
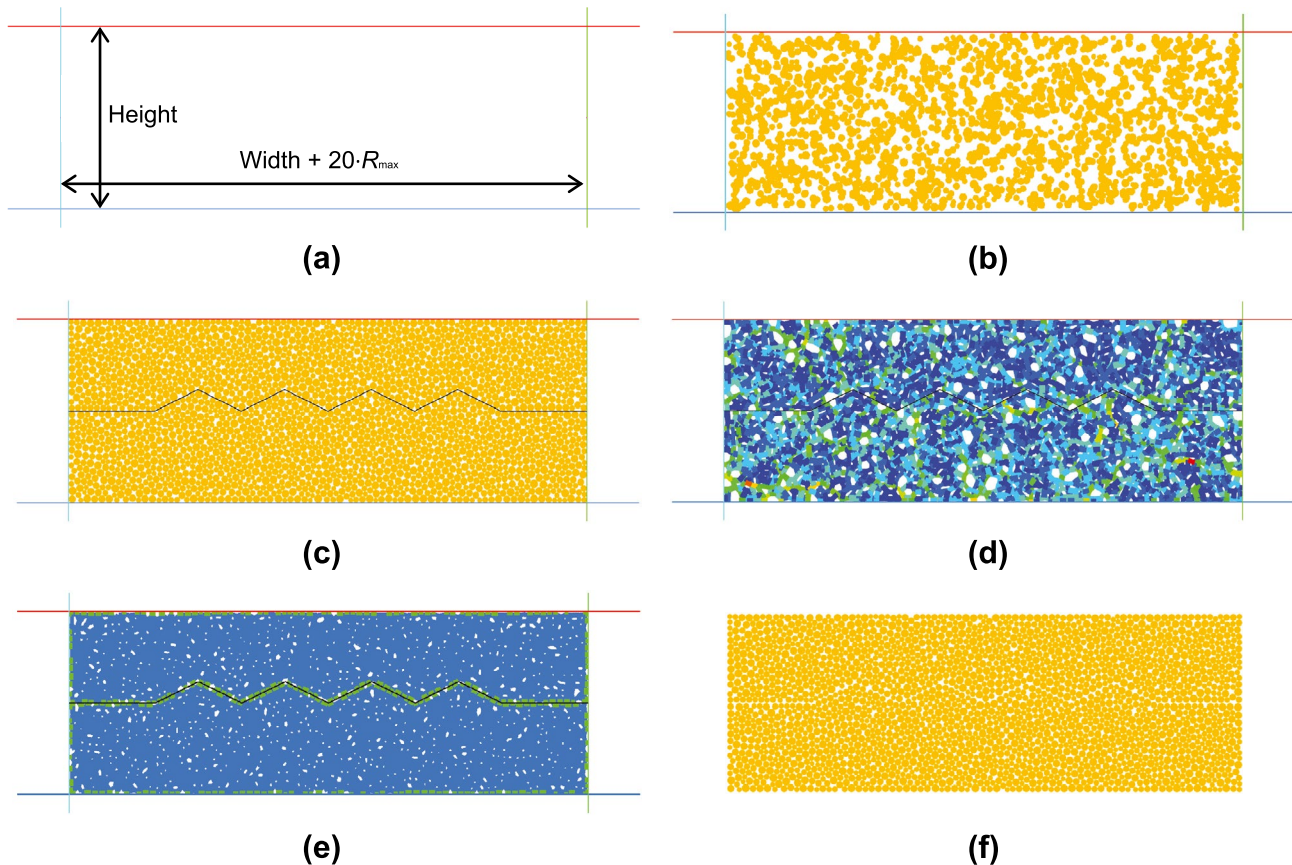
Numerical shear test environment in PFC^{2D}

The numerical shear test environment in PFC^{2D} presented in this paper follows a procedure similar to the specimen generation procedure for the SBG approach suggested by Bahaaddini et al. (2013), which aims to avoid interlocking between particles. However, there are three main differences between the SBG approach described in Bahaaddini et al. (2013) and the shear test environment developed in PFC^{2D} Version 5 (Itasca 2018) presented in this study. First, only one wall representing the joint profile is inserted to divide the assembly of particles into two parts in the specimen generation step. The SBG approach by Bahaaddini et al. (2013), on the other hand, divides the numerical rock

sample into two parts by inserting two walls that follow the joint profile. Second, the elimination of floating particles is not carried out in the numerical shear test environment presented in this paper. Instead, a predefined installation gap ensures that parallel bonds are installed at each particle–particle contact. Furthermore, the elimination of floaters is not available in the PFC version used in this study, since it was replaced by this new approach (i.e., installation gap). Third, the stress measurements during the installation of the isotropic stress are carried out on the whole upper and lower parts of the specimen separately. The mean stress in the methodology described by Bahaaddini et al. (2013) was measured by setting five measurement circles in each part of the rock sample.

The modelling procedure in the shear test environment in PFC^{2D} presented in this study involves the following four steps:

1. *Specimen generation*: In the first step, the generation of the rock assembly is carried out in six different substeps, as illustrated in Fig. 1a-f:

Fig. 1 Specimen generation procedure in the numerical shear test environment: **a** vessel generation; **b** grain assembly; **c** joint wall generation; **d** isotropic stress installation; **e** Parallel bond installation; **f** specimen removed from vessel

(a) The material vessel consisting of four walls defining a rectangle in 2D with a specific width and height is generated. The total width of the vessel is determined by adding an extra length of twenty times the maximum particle radius (R_{max}) to the actual width of the rock joint sample (see Fig. 1a).

(b) In the second sub-step, the vessel is filled with an assembly of particles located in random positions (see Fig. 1b). The size of the particles varies between the range of the defined minimum particle radius (R_{min}) and R_{max} satisfying a uniform size distribution. The number of particles depends on the volume of the material vessel, the grain size distribution, and the overall grain porosity (n_c), respectively. The n_c value used in the numerical simulations in PFC^{2D} aims at obtaining a well packed assembly of particles, and it is not the porosity of the actual rock material. The material-modelling support in PFC recommends a n_c value of 0.08 for simulations in 2D (Potyondy 2018a).

(c) The assembly of particles is then divided into two parts, upper and lower, by inserting a wall that follows the joint profile. This is illustrated in Fig. 1c. The particles are allowed to freely rearrange separately in the upper and lower parts under the condition of zero friction, interacting also with the wall that represents the joint profile. The kinetic energy in the numerical simulations is dissipated via the local damping factor available in PFC^{2D}. This local damping factor is equal to 0.7 to approximate quasi-static conditions (Potyondy 2018a).

(d) The specified isotropic stress is applied in the upper and lower parts of the numerical specimen as if they were independent samples using the grain-scaling procedure described in Potyondy (2018a) (see Fig. 1d). The particle sizes are scaled iteratively until the target stress (0.1 MPa) was within tolerance (0.01 Pa) in both parts. Furthermore, the particles in the upper and lower parts, respectively, are identified by assigning a different zone ID. The zone ID is set to 1 for particles in the upper part and to 2 for particles in the lower part.

(e) Parallel bonds are installed at each particle–particle contact with an installation gap less than or equal to 30% of the R_{min} value, as illustrated in Fig. 1e. The aim of the installation gap is to ensure that no particles are left without a parallel bond at the end of the specimen generation procedure (i.e., floating particles).

(f) Finally, the specimen is removed from the material vessel. The walls defining the vessel and the joint profile are deleted, as illustrated in Fig. 1f.

2. *Smooth-joint contact installation*: In the second step, the joint is inserted in the numerical rock specimen by assigning SJCM to all particle–particle contacts intersected by the joint profile, as illustrated in Fig. 2a. The SJCM installation performed in the shear test environment in this study uses the discrete fracture network (DFN) logic embedded in PFC^{2D}. Thus, each segment of the rock joint profile is represented by a DFN joint, which is identified by an ID number different to zero. This ID number is used to assign the properties of a specific DFN joint to the SJCM generated by that joint segment. The normal vector of the SJCM assigned to each particle–particle contacts intersected by the joint profile is always directed normal to the joint fragment. For the case of particle–particle contact, the normal vector is directed along the line between their respective centres (Itasca 2018). In the case that the contact between two particles is intersected by two DFN joints, the installed SJCM corresponds the joint segment to the left of the contact. This is, however, a rare case that can be prevented with an appropriate particle resolution (P_{res}).

3. *Seating phase*: In the third step, the specified σ_n is applied to the upper part of the numerical specimen. Additionally, the left and right sides of the upper part of the rock specimen are carved, exposing two wings in the lower part (see Fig. 2a). The value assigned to the width of each carved wing is ten times the R_{max}. The main purpose of the wings is to provide continuity to the joint and to prevent the upper part from bending after large horizontal displacements during the numerical direct shear tests. Furthermore, four walls are installed to provide the boundary conditions to the numerical specimen. The lower sample is fitted in a box defined by three fixed walls and a top wall is installed over the upper part. The σ_n is applied by means of a servo-control mechanism installed on the top wall, making it constant during the numerical shear test. The servomechanism used in the numerical simulations in this study is a procedure available in PFC^{2D} that provides the ability to control the velocity of the top wall to apply or maintain a certain level of σ_n (Itasca 2018; Potyondy 2018a). During the seating phase, the upper part of the specimen is compressed downwards until the applied σ_n is within the specified tolerance. This process may lead to the generation of new contacts between both parts of the sample at the joint profile location. In this phase, the SJCM's installation is managed by the joint profile location defined by the DFN joint, as explained in step 2. Therefore, since the SJCM's installation is still active in this step, the SJCM is assigned to the new contacts created.

Fig. 2 Numerical rock joint specimen with saw-tooth asperities after SJCM installations: **a** prior the numerical shear test with carved wings and installed walls providing boundary conditions. The zoom in around the saw-tooth joint profile illustrates the two layers of particles defined by the ball extra variable 1 (magenta colour), the SJCM between particles on both sides of the joint profile (green colour), and the particles located further away from the joint profile with installed parallel bonds (blue colour); **b** during the numerical shear test with defined left and right grips simulating an actual laboratory test
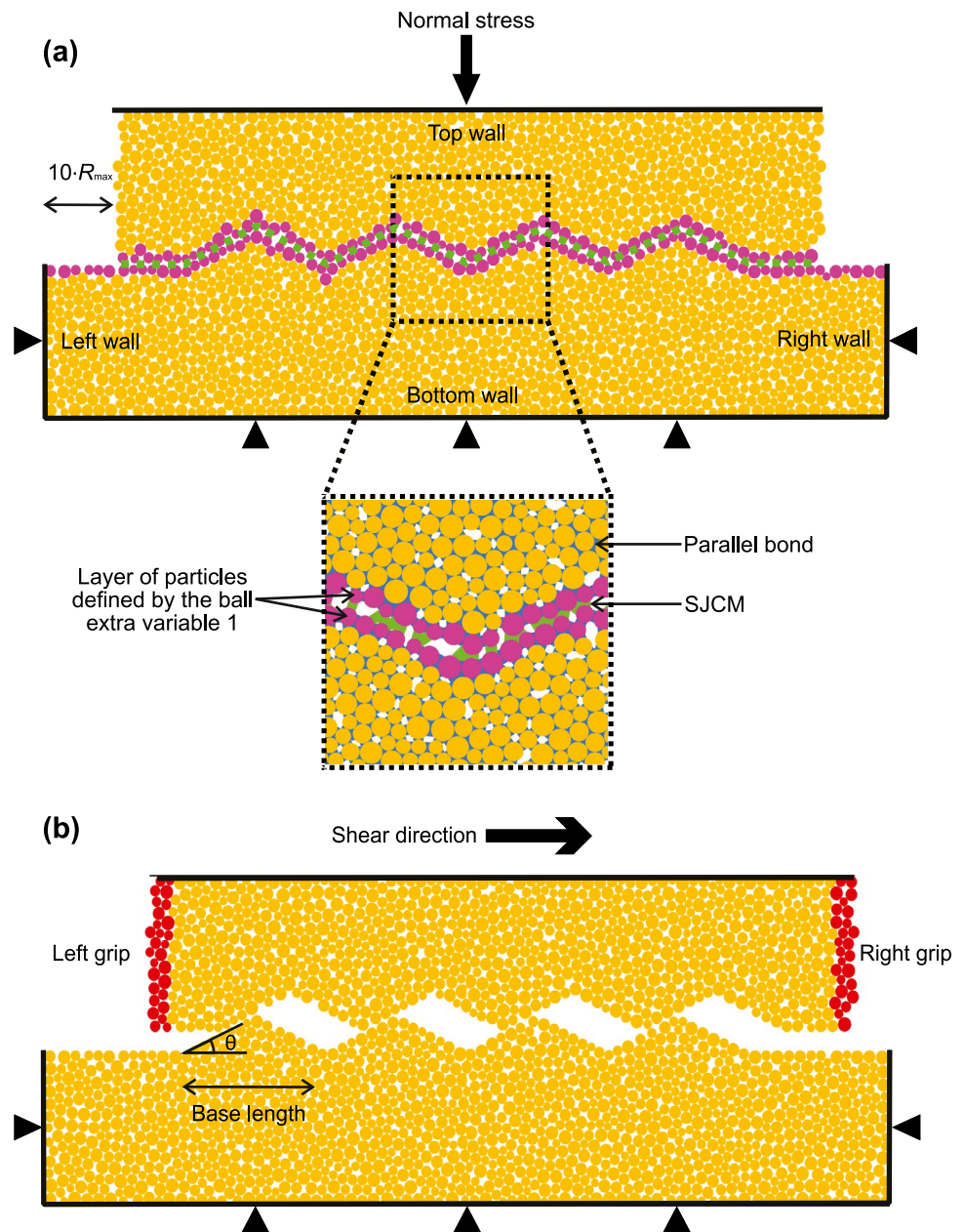
4. *Direct shear test*: In the final step, the specimen is ready to be tested in the numerical shear test environment. Prior to the numerical shear testing, the DFN ID assigned in the SJCM installation is stored in the contact variable 1, thus pointing out the joint segment where the SJCM is located. Furthermore, the ball extra variable 1 is defined to store the ID of the closest DFN-joint to a certain particle, provided that the distance between the particle's perimeter and the DFN-joint is less than a specified tolerance set by default to R_{max}. This is illustrated in Fig. 2a. The ball extra variable 1 defines two layers of particles above and below the joint profiles' boundary that is used to assign SJCM to new created contacts during the numerical shear tests. A new SJCM is installed at a new generated contact during a numerical test if the ball extra variable 1 of any of the particles defining the contact is set to a value different to zero; otherwise, a parallel bond will be assigned to the contact. The assigned properties of the SJCM correspond with the DFN ID stored in the ball extra variable 1 of the particle further away from the driving grip (i.e., where the velocity is applied). To simulate a laboratory direct shear test, two grips are defined at the left and right sides of the upper part of the specimen. The grip thickness is set to 1.5 times the R_{max}. This is illustrated in Fig. 2b. The velocity is gradually applied to the right, or left,

grip until a maximum value of 0.05 m/s is reached in the numerical direct shear test. This velocity in the shear test environment in PFC^{2D} is low enough to ensure that the sample remains in quasi-static equilibrium. Furthermore, the gradual application of shear velocity in the numerical simulations reduces the possibility of having a dynamic compression wave in the upper part of the numerical specimen.

There are, however, still situations, such as when applying high σ_n or after the upper part has undergone a considerable shear displacement (more than one particle diameter), in which the generation method alone is not sufficient with respect to interlocking. This issue has also been discussed by Mehranpour and Kulatilake (2017) and Li et al. (2020). During the initial trial simulations with high applied σ_n, it was observed that particles on both sides of the joint profile with SJCM were pushed against each other, thus generating large stress concentrations. The observed particle interlocking due to overlapping was remedied in this study by increasing the SJCM's normal stiffness (k_n) to a constant value based on the uniaxial compressive strength of the intact rock (σ_{ci}), given by

$$k_n = \frac{\sigma_{ci}}{2 \cdot R_{avg}},\tag{1}$$

where R_{avg} is the average particle radius in the numerical specimen.

Calibration of the intact rock and smooth-joint contact model parameters

Intact rock parameters

The intact rock material utilised in the numerical shear tests presented in this study was generated with the material-modelling package functions provided in PFC^{2D} using parallel bonded material (PBM) (Potyondy and Cundall 2004; Potyondy 2018a). The micro-properties of the PBM were calibrated against the intact rock properties of a granite rock joint sample previously tested in the laboratory by Johansson (2016). The rock material came from the Flivik quarry in Sweden and consisted of grey coarse-grained granite. The measured macro-properties of the intact granite rock are provided in Table 1.

In PFC^{2D}, a series of numerical uniaxial compressive strength (UCS) tests was conducted to match the σ_{ci}, Young's modulus (E_i) and Poisson's ratio (v_i) of the intact material measured in the laboratory. The numerical specimens generated in the UCS tests had a width of 50 mm and a height of 100 mm (see Fig. 3a). The specimen generation procedure in

Table 1 Macro-properties of the intact granite rock measured in the laboratory by Johansson (2016) and simulated in PFC^{2D} with a P_{res} of 6 particles per numerical specimen width

		σ_{ci} [MPa]	E_i [GPa]	v_i [-]
Experimental	Average	197	84	0.26
PFC^{2D}	Average	197.8	84.2	0.25
	SD	45.9	5.9	0.03
	COV (%)	23.2	7	12

the numerical UCS tests is similar to the generation procedure of the shear test environment described in section "Numerical shear test environment in PFC^{2D}". However, the shear test environment generates the upper and lower parts of the numerical rock specimen as two independent materials. To create the rock assembly, the rectangular vessels (2D) were filled with particles with a R_{min} of 2.88 mm and a n_c value of 0.08. The particle size distribution was assigned as uniform with a $R_{max} = 1.66 \cdot R_{min}$. This relationship gives a R_{avg} of 3.83 mm and a P_{res} of 6 particles per numerical specimen width. This adopted P_{res} value aimed at finding a trade-off between modelling the surface roughness, the asperity strength of the actual rock joint sample, and computational effort. Parallel bonds were also installed at each particle–particle contact with an installation gap less than or equal to 30% of the R_{min} value. To capture the strength variability of the PBM due to different particle packing arrangements, a series of material realisations was created and tested by varying the seed value of random-number generator (S_{RN}). Figure 3b illustrates the failure of one of the generated specimens during the UCS tests performed. The results of the deviator stress and radial strain versus axial strain obtained in the numerical UCS tests with different values of S_{RN} are presented in Fig. 4. The average value, standard deviation (SD), and coefficient of variation (COV) of the simulated macro-properties in PFC^{2D} are presented in Table 1. The calibrated micro-properties of the PBM are provided in Table 2. The parallel bonds with properties in Table 2 installed at each particle–particle contact provide the behaviour of two interfaces (Potyondy 2018a). The first interface is equivalent to the linear elastic model, and the second interface is the parallel bond. When the second interface is bonded, it resists relative rotation and its behaviour is linear elastic until the strength limit is exceeded.

Smooth-joint contact model parameters

During the numerical direct shear tests performed in PFC^{2D}, the SJCM was assigned to all particle–particle contacts intersected by the modelled rock joint profile. The SJCM parameters utilised in this study are based on results from three laboratory direct shear tests on sawn, planar rock joints performed by Lazzari et al. (2014) corresponding to

Fig. 3 Numerical specimen generated in PFC^{2D} to conduct the UCS tests: **a** before the test starts; **b** after reaching the point of failure in the specimen. The red and black colours indicate tensile and shear failure, respectively
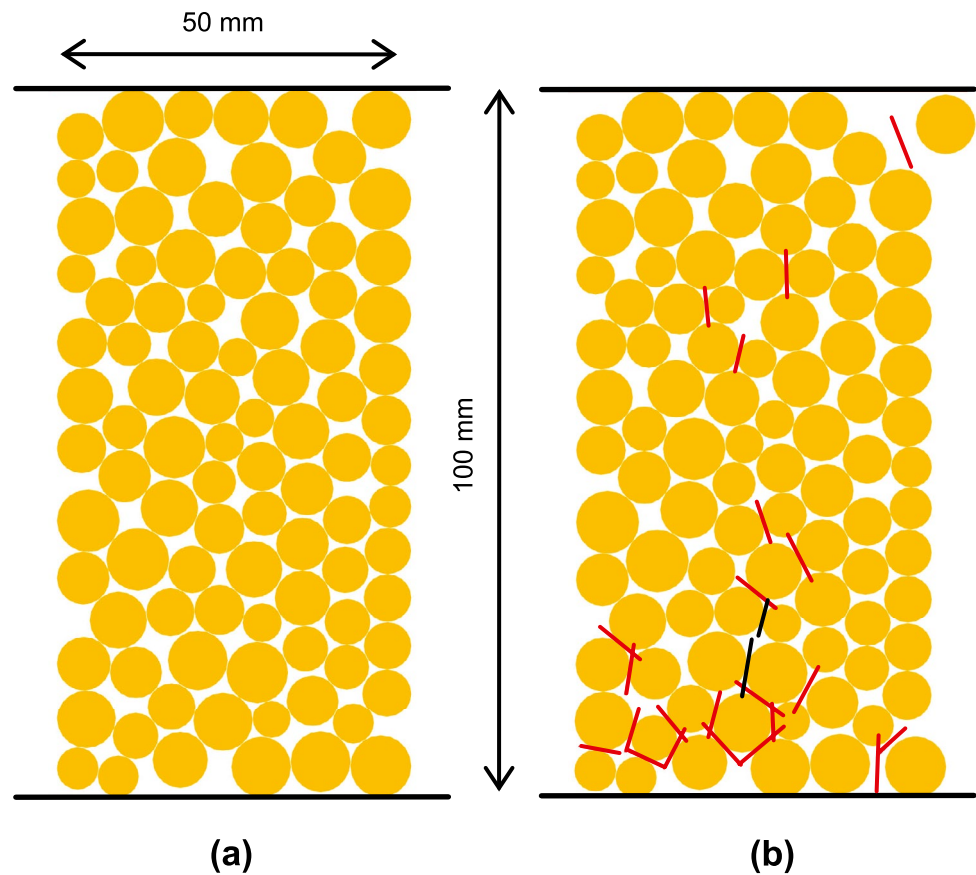
the basic friction angle. The three laboratory samples had a length of 60 mm, and they were of the same type of granite from the same quarry as utilised by Johansson (2016) in the laboratory direct shear tests. The numerical simulations performed by Lazzari et al. (2014) to calibrate the properties of the SJCM had a R_{min} of 0.38 mm and a R_{max} of 0.62 mm, respectively. The SJCM parameters used in this study correspond to the macro-properties of the joint profile segments, which are independent of particle size. The exception in this study is the value of k_n derived with Eq. (1) to prevent interlocking between particles. The values of the calibrated parameters of the SJCM utilised in the numerical simulations in PFC^{2D} are presented in Table 3. The friction coefficient of the SJCM is assumed to be constant in the numerical direct shear tests performed in this study.

Verification of the shear test environment in PFC^{2D} with idealised, saw-tooth triangular joint profiles

To check the applicability of the shear test environment in PFC^{2D} presented in this study to simulate the shear strength of rock joints, a series of numerical direct shear tests on rock joints with idealised, saw-tooth triangular asperities

was conducted under constant normal load (CNL) conditions with different applied σ_n. Furthermore, the peak shear strength of the idealised joint profiles obtained in the numerical calculations in PFC^{2D} was compared with the peak shear strength obtained analytically using the criteria developed by Patton (1966) and Ladanyi and Archambault (1969). These two criteria were originally developed by studying the mechanical behaviour of rock joints with idealised, saw-tooth asperities.

The numerical specimens created in PFC^{2D} had a width of 100 mm and a height of 40 mm. Three different saw-tooth triangular joint profiles with a dip angle (θ) of 15°, 25° and 35° were tested under different applied σ_n (1, 2, 3, 5 and 10 MPa). These values of θ are similar to the ones utilised in the study by Bahaaddini et al. (2013) and were chosen to capture both sliding over and shearing through the asperities. The base length of the saw-tooth asperities in the numerical specimens was 20 mm. Figure 2 shows one of the tested numerical specimens with saw-tooth asperities and a θ of 25°. The rock assembly was created by filling the rectangular vessels (2D) with particles with a R_{avg} of 0.8 mm and a n_c of 0.08. The particle packing arrangement of all generated numerical specimens was created with the same S_{RN} = 10,001. As in the UCS tests performed, the relationship between R_{min} and R_{max} was 1.66. On average, each asperity of the saw-tooth
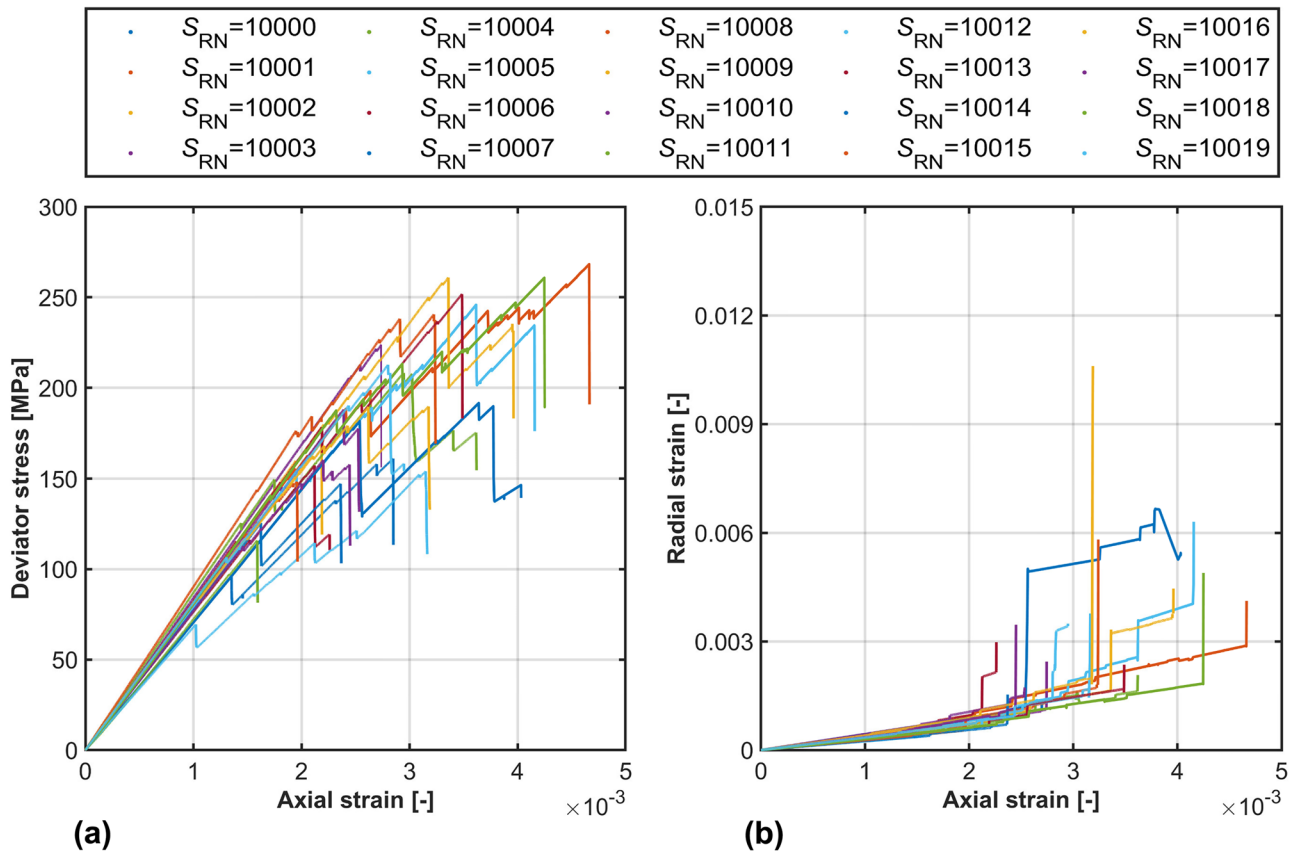
Fig. 4 Results of the numerical UCS tests on the numerical specimens generated with different values of S_{RN}: **a** deviator stress vs. axial strain; **b** radial strain vs. axial strain

joint profile had a P_{res} of 6 particles. This is similar to the P_{res} of the generated numerical specimens in the UCS tests for the calibration of the micro-properties of the PBM. In the calibration process shown in section "Calibration of the intact rock and smooth-joint contact model parameters", it is the number of particles (i.e., P_{res}) perpendicular to the application of the major principal stress that governs the simulated macro-properties of the numerical UCS tests, rather than the particle radius. The micro-parameters of the PBM and installed SJCM are provided in Tables 2 and 3. The results of shear stress (τ) versus shear displacement (δ_s) for all the direct shear tests performed in PFC^{2D} are illustrated in Fig. 5a-c.

The comparison made between τ and δ_s shows that for all the tested saw-tooth profiles the peak shear stress (τ_p)

increases with higher values of σ_n. The values of shear displacement at peak (δ_p) also increase with higher values of σ_n. Furthermore, the results of the direct shear tests performed show that sliding failure controls the shearing process. The exception is the saw-tooth joint profile with $\theta = 35°$. In this joint profile, a higher number of tensile and shear cracks could be observed on the surface of the triangular asperities in the simulated shear tests with σ_n higher than 1 MPa (see Fig. 6a-c). This observed mechanical behaviour in the numerical direct shear tests on rock joints with idealised, saw-tooth asperities is consistent with other results reported in the literature by Bahaaddini et al. (2013) and Li et al. (2020).

The values of τ_p obtained in the numerical simulations under the different applied σ_n were then compared to the τ_p

Table 2 Calibrated micro-properties of the PBM obtained in the numerical UCS tests in PFC^{2D} with a P_{res} of 6 particles per numerical specimen width

Particle properties		Parallel bond properties	
Particle density [kg/m^3]	2660	Young's modulus [GPa]	77.5
Young's modulus [GPa]	77.5	Cohesive strength [MPa]	116 ± 23.2
Friction coefficient [-]	2.5	Tensile strength [MPa]	116 ± 23.2
Normal to shear stiffness ratio [-]	5.0	Normal to shear stiffness ratio [-]	5.0

Table 3 Calibrated SJCM parameters used in the numerical shear test simulations in PFC[2D]

SJCM parameters	
Normal stiffness [GPa/m][a]	1250
Shear stiffness [GPa/m]	7
Friction coefficient [-]	0.61

[a]Value obtained using Eq. (1) with R_{avg} of 0.08 mm

obtained analytically with the shear strength criteria developed by Patton (1966), and Ladanyi and Archambault (1969). Based on the observations made in Figs. 5a-c and 6a-c on the predominant failure mode controlling the shearing process, only the part of Patton's failure criterion accounting for sliding failure was used. The shear strength criteria of Patton (1966) and Ladanyi and Archambault (1969) can be expressed as:

$$\tau_p = \sigma_n \tan\left(\phi_b + i\right), \tag{2}$$

and

$$\tau_p = \frac{\sigma_n\left(1 - a_s\right)\left(\dot{v} + \tan\phi_b\right) + a_s\sigma_{ci}}{1 - \left(1 - a_s\right)\dot{v}\tan\phi_b}, \tag{3}$$

where ϕ_b is the basic friction angle, i is the inclination of the saw-tooth asperities with respect to the shear direction, a_s is the shear area ratio and $\dot{v}$ is the rate of dilation at failure. The value of ϕ_b of the tested granite rock material is 31.4°.

The comparison between the τ_p simulated in PFC[2D] and that calculated with Eqs. (2) and (3) is illustrated in Fig. 5d-f. The values of τ_p simulated in PFC[2D] were in good agreement with the τ_p calculated with Patton (1966) and Ladanyi and Archambault (1969). This shows that the shear test environment in PFC[2D] presented in this study can simulate the mechanical behaviour of rock joints with idealised, saw-tooth asperities with applied values of σ_n up to 10 MPa. The reason for the observed discrepancies between predicted τ_p with the criteria of Patton (1966) and Ladanyi and Archambault (1969) in Fig. 5d and e, respectively, is that sliding failure controls the shearing process for the tested rock material at low θ values. The criterion by Ladanyi and Archambault (1969) accounts for the contribution from both sliding and shearing based on energy principles. However, at higher inclinations (i.e., $\theta = 35°$ in Fig. 5f), shearing through the asperities starts to occur. The contribution from shearing through the asperities is taken into account in Ladanyi and Archambault's peak shear strength criterion, and therefore, the simulated τ_p has a better agreement with the predicted τ_p using Eq. (3) for this value of θ.

Numerical direct shear test in PFC[2D] of an actual rock joint in granite

Rock joint sample and joint profile geometry

The shear test environment in PFC[2D] was utilised to simulate the peak shear strength of an actual rock joint obtained in laboratory testing. A tensile-induced rock joint sample in grey coarse-grained granite with dimensions of 60 by 60 mm, previously tested in the laboratory under CNL conditions by Johansson (2016), was utilised in this study. A comparison was made between the results of the laboratory and numerical direct shear tests performed with an applied σ_n of 1 MPa.
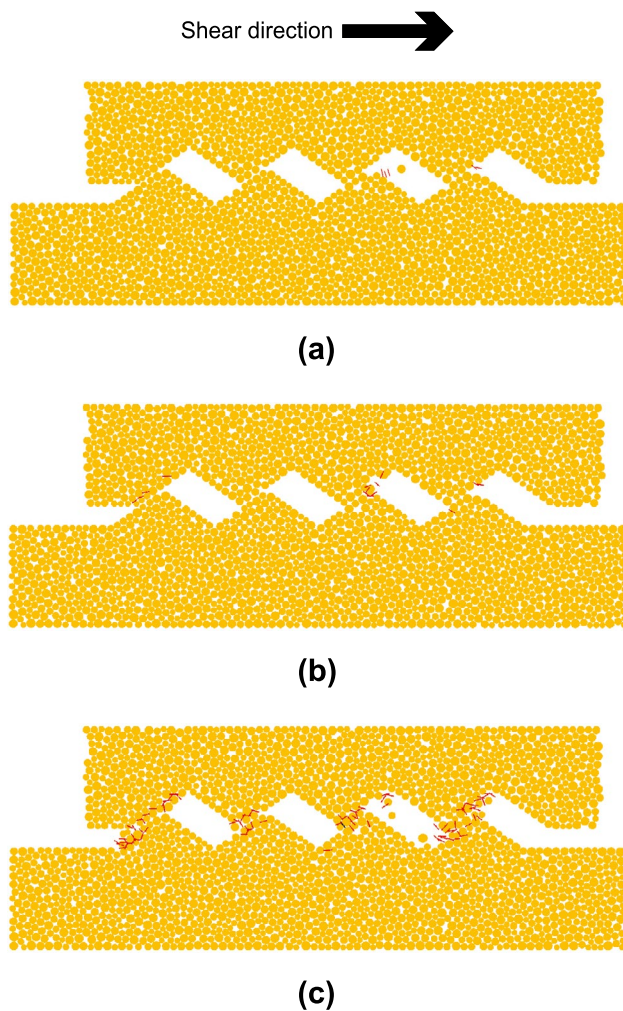
The numerical direct shear tests in PFC[2D] were performed on three different two-dimensional profiles selected along the shear direction in the actual rock joint. These joint profiles were selected after studying the high-resolution optical scanning measurements of the surface roughness. The scanning measurements were taken with an ATOS III system and are presented in Johansson (2016). The measurements had a resolution of approximately 120–140 μm. The scanned surface was regenerated with a resolution of 0.3 by 0.3 mm. This selected resolution was based on the observations made in the laboratory by Johansson (2016) on the mechanical behaviour of the perfectly mated rock joint samples tested. He observed that, on average, the measured value of δ_p in these samples was approximately 0.3 mm. He concluded that this gives an indication of the size of the effective asperities contributing to the shear strength at the peak. Furthermore, the resolution of 0.3 by 0.3 mm is assumed to be appropriate to capture the grain size according to previous recommendations by Grasselli and Egger (2003), and Tatone and Grasselli (2009). The first joint profile (2D) was selected in the centre of the analysed sample. The second and third profiles were selected at approximately the centre of the left and right remaining halves, respectively. In addition, profile 3 was taken along the asperity with maximum value of apparent dip angle facing the shear direction (θ^*). The digitised rock joint surface in three dimensions and the three two-dimensional profiles tested in the numerical shear test environment in PFC[2D] are illustrated in Fig. 7. To be consistent with the laboratory observations from Johansson (2016) and to achieve a good representation of the surface roughness in PFC[2D], the joint profiles in the numerical direct shear tests had a segment length (SL) of 0.3 mm. The shear direction indicated in Fig. 7 refers to the shear direction of the lower parts of the tested numerical rock specimens.
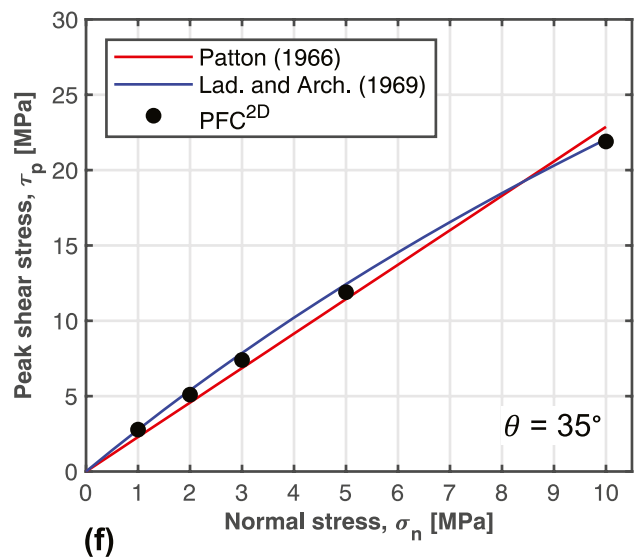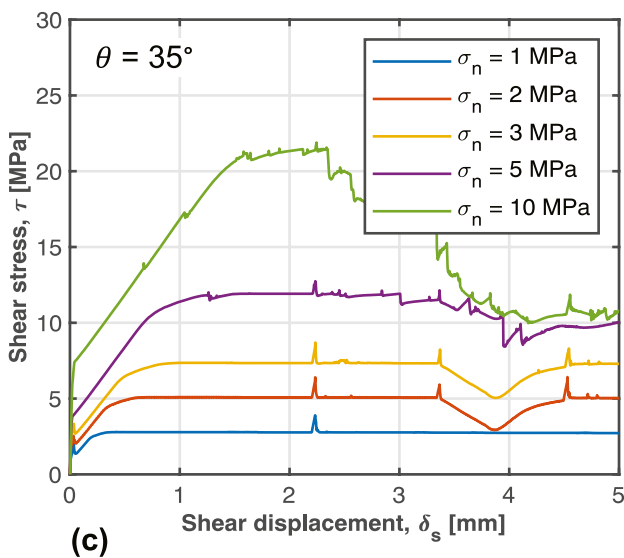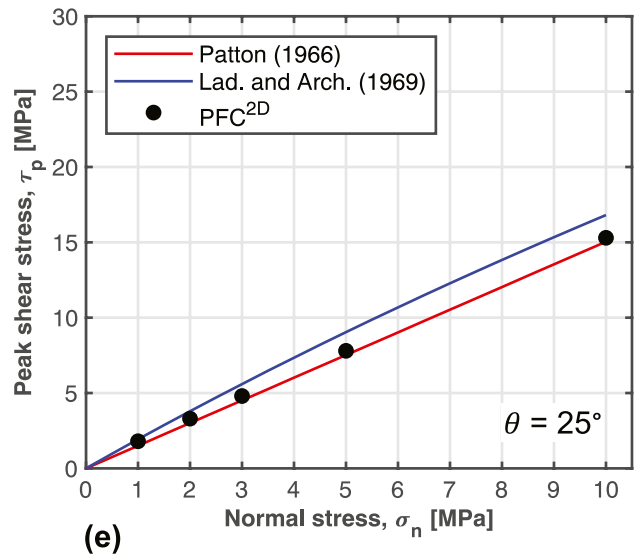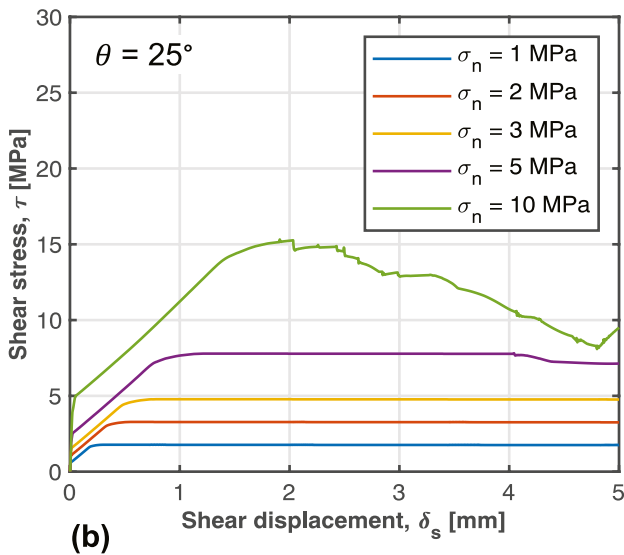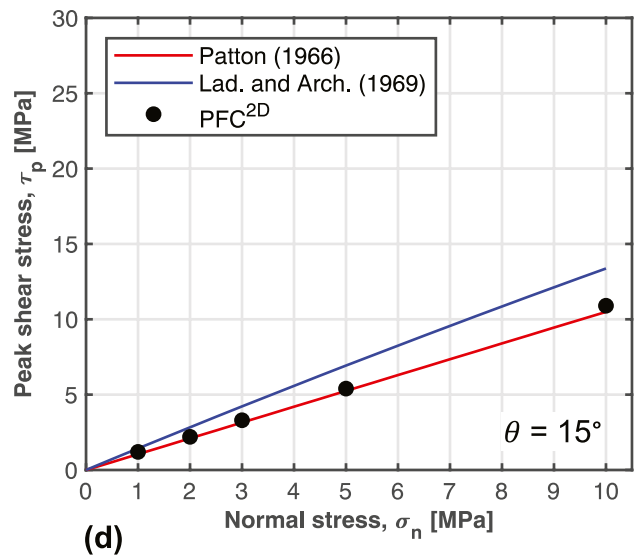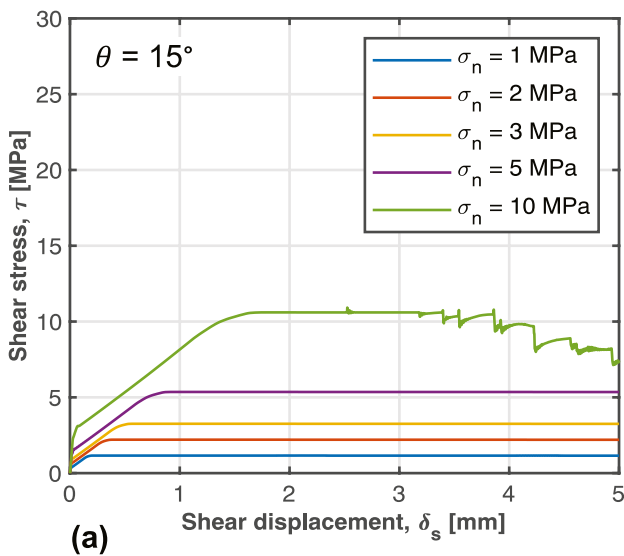
◄**Fig. 5** Results of the numerical shear tests on the rock joint specimens with idealised, saw-tooth asperities with different applied values of σ_n, and comparison with the analytical criteria by Patton (1966), and Ladanyi and Archambault (1969): shear stress, τ vs. shear displacement, δ_s with **a** $\theta = 15°$; **b** $\theta = 25°$; **c** $\theta = 35°$; and peak shear stress, τ_p vs. normal stress, σ_n with **d** $\theta = 15°$; **e** $\theta = 25°$; **f** $\theta = 35°$

Shear test simulations

The numerical specimens created in PFC^{2D} to test the three different joint profiles had a width of 60 mm and a height of 15 mm. The relationship between height and width (1:4) was based on a preliminary sensitivity analysis in the shear test environment intended to find the optimal sample size that numerically simulates stable shear behaviour without cracking the samples and at the same time be calculated within a reasonable computational time.


(a)

(b)

(c)

Fig. 6 Asperity degradation during the numerical direct shear tests in PFC^{2D} on the rock joint samples with saw-tooth asperities with $\theta = 35°$ after a δ_s of 5 mm: **a** $\sigma_n = 1$ MPa; **b** $\sigma_n = 3$ MPa; **c** $\sigma_n = 10$ MPa. The red and black colours indicate tensile and shear failure, respectively

The roughness resolution in the simulated rock joint in PFC^{2D} depends on the magnitude of SL and P_{res} in each segment. In the numerical shear tests performed, the rectangular vessels were filled with particles with a R_{avg} of 0.08 mm. The relationship between R_{min} and R_{max} was 1.66. The particle packing arrangement of the three numerical specimens was created with the same $S_{RN} = 10001$. On average, each segment of the tested joint profiles had a P_{res} of approximately 2 particles. This P_{res} differs from the one utilised in both the UCS tests in section "Calibration of the intact rock and smooth-joint contact model parameters" and the direct shear tests with the saw-tooth profiles in section "Verification of the shear test environment in PFC^{2D} with idealised, saw-tooth triangular joint profiles". This was mainly due to limitations in the computational time. To further reduce the numerical instabilities when using small particle radius, a scaling algorithm was used where the particle radius and the dimensions of the numerical shear test were scaled with a factor of 20. The generation and direct shear test procedures in PFC^{2D} of the numerical specimens follow the principles explained in section "Numerical shear test environment in PFC^{2D}". Furthermore, the upper parts of the numerical specimens were sheared in the same direction as the laboratory shear tests (from left to right) by gradually applying velocity on the left grip (see Fig. 8). The σ_n applied during the numerical direct shear tests was equal to 1 MPa, as in the laboratory test. The micro-parameters of the PBM and properties of the SJCM installed in the numerical shear tests are provided in Tables 2 and 3.

A comparison between the results from the laboratory direct shear test and the numerical simulations in PFC^{2D} on the selected joint profiles in the form of mobilised friction angle (ϕ) versus δ_s is presented in Fig. 9. The values of ϕ are calculated from the recorded values of τ and σ_n during the numerical simulations in PFC^{2D}, which is given by

$$\phi = arctan\left(\frac{\tau}{\sigma_n}\right). \tag{4}$$

The measured mobilised peak friction angle (ϕ_p) of the rock joint sample tested in the laboratory by Johansson (2016) was 65°. The results of the numerical direct shear tests with profiles 1, 2 and 3 showed a ϕ_p of 52.8°, 58.2° and 65.8°, respectively. The ϕ_p of profile 3 simulated in PFC^{2D} was 13° and 7.6° higher than the ϕ_p of profiles 1 and 2, respectively. The difference between the ϕ_p measured in the laboratory and that simulated in PFC^{2D}, as expressed in absolute values, varied between 0.8° and 12.2°. The measured post-peak ϕ in the laboratory test after a δ_s of 1.5 mm was 52°. The post-peak ϕ of profiles 1, 2, and 3 simulated in PFC^{2D} after a δ_s of 1.5 mm was 24°, 38°, and 33°, respectively. The difference between measured post-peak ϕ in the laboratory and simulated in PFC^{2D} varied between 14° and 28°. The measured δ_p

(a)

(b)
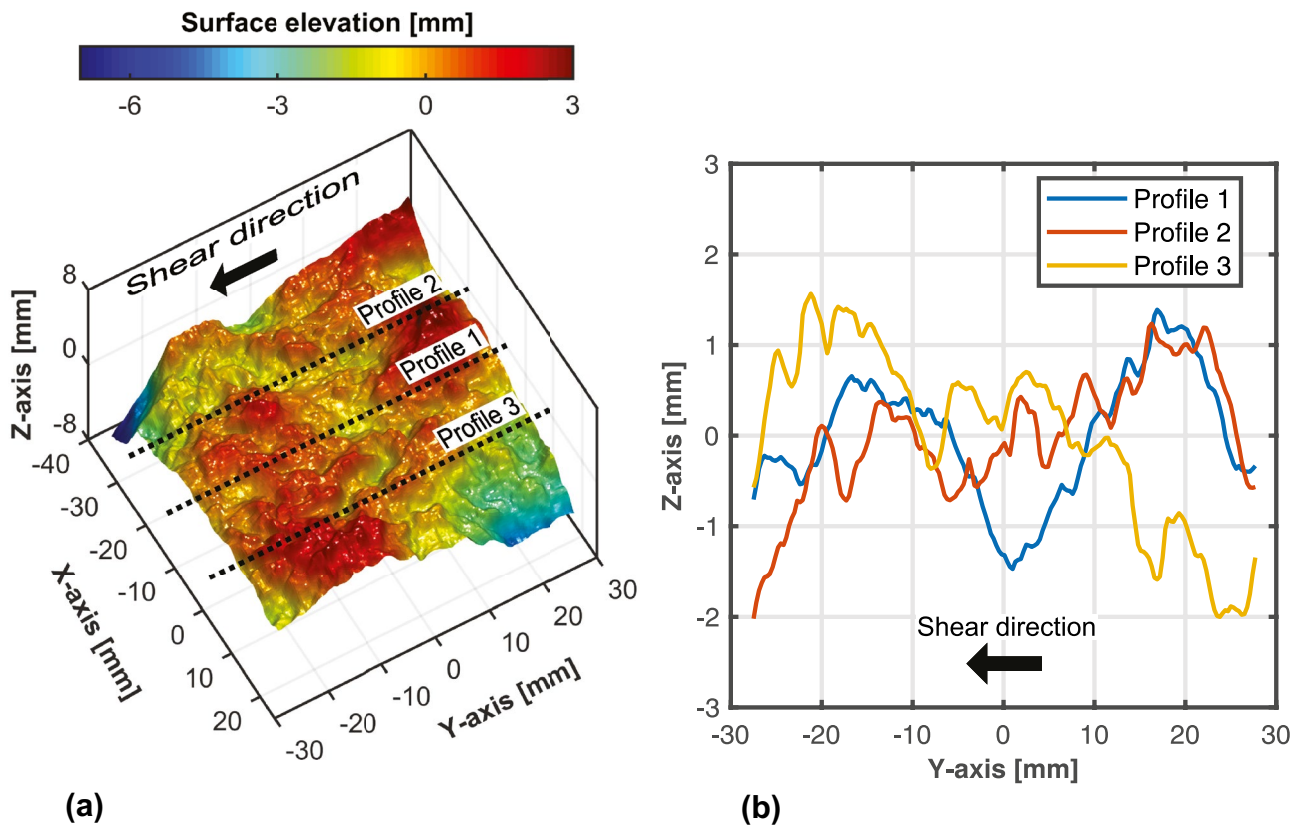
Fig. 7 a Digitised rock joint surface with dimensions of 60 by 60 mm obtained from the performed optical scanning measurements with a resolution of 0.3 by 0.3 mm; **b** Rock joint profiles tested in the numerical direct shear tests in PFC^{2D} selected along the shear direction with a SL of 0.3 mm. Profile 3 passes through the asperity with maximum measured θ^*

of the laboratory test was 0.35 mm. The values of δ_p in the numerical simulations with profiles 1, 2, and 3 were 0.41, 0.18, and 0.15 mm, respectively.

The numerical direct shear tests in PFC^{2D} performed on profiles 1, 2, and 3 after a δ_s of 1.5 mm is illustrated in Fig. 8. The results of the numerical shear tests showed that sliding failure mostly controlled the shearing process in PFC^{2D}. There were, however, some areas along the tested joint profiles where tensile and shear cracking could be observed. These cracks developed superficially and were located in those areas where the asperities are steeper, i.e., higher values of θ^*. These results from the numerical simulations agree with the observations made by Johansson (2016) on the actual rock joint tested in the laboratory.

Discussion

Numerical shear tests in PFC^{2D} with actual rock joint profiles

The obtained results of the numerical direct shear tests performed in PFC^{2D} with profiles 1, 2, and 3 show that the shear

test environment, together with the methodology presented in this study, has the capability of realistically capturing the principal shear behaviour of actual hard crystalline rock joints under the applied value of σ_n.
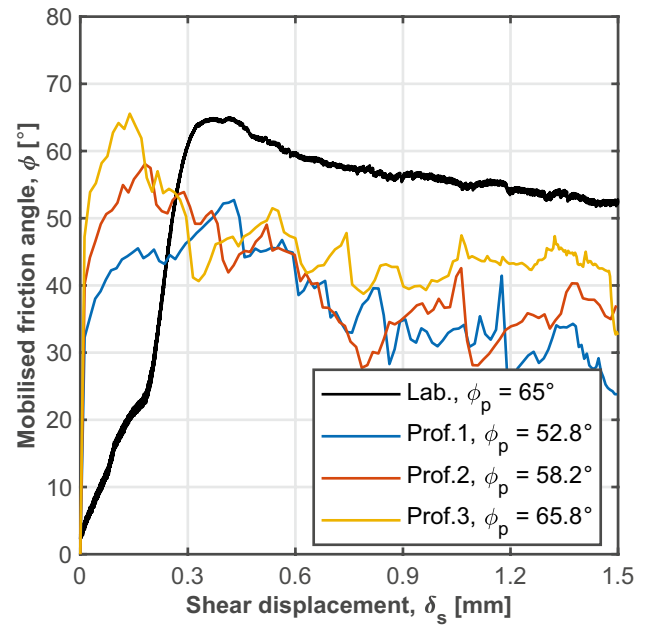
From a qualitative point of view, the three joint profiles captured well the peak and post-peak behaviour compared with the actual analysed rock joint. Furthermore, the results obtained in the numerical shear tests indicate that the effect of increasing the k_n of the SJCM as in Eq. (1) has a negligible influence on the simulated peak shear strength of the tested rock joint profiles. However, the elastic part of the stress-shear displacement curve could be slightly influenced by this assumption, due to the contribution of the local normal stiffness of the asperities to the overall shear stiffness of the sample (see Figs. 5 and 9). From a quantitative point of view, only profile 3, which was taken through the steepest asperity, was in reasonably good agreement when comparing its ϕ_p simulated in PFC^{2D} with that measured in the laboratory. However, it is still uncertain if the number of contact points generated in a joint profile in 2D containing the steepest asperity can capture the three-dimensional characteristics of surface roughness of actual rock joints. A three-dimensional approach may therefore capture the actual

Shear direction

(a)

(b)

(c)
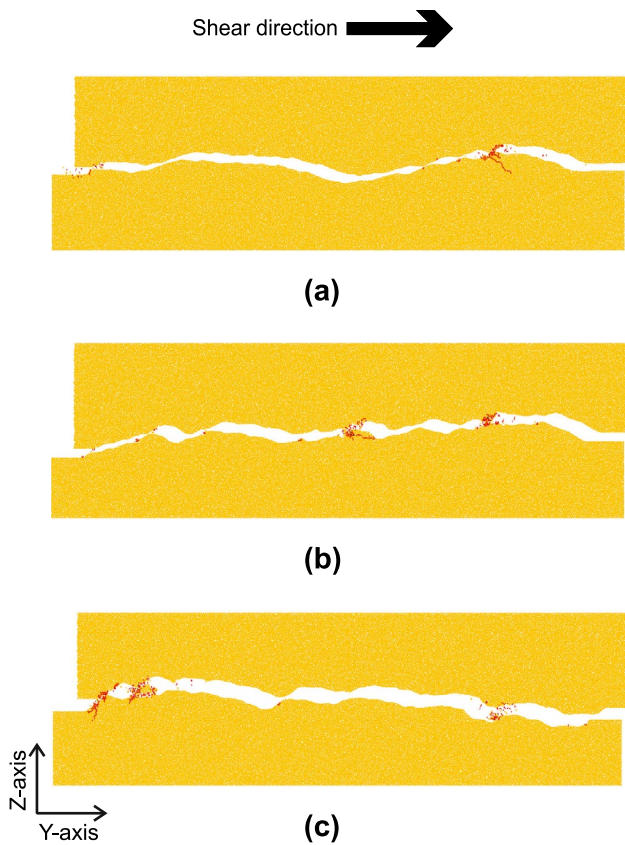
Fig. 8 Asperity degradation during the numerical direct shear tests in PFC^{2D} with an applied σ_n of 1 MPa on the selected rock joint profiles after a δ_s of 1.5 mm: **a** profile 1; **b** profile 2; **c** profile 3. The red and black colours indicate tensile and shear failure, respectively

Fig. 9 Results of mobilised friction angle, ϕ vs. shear displacement, δ_s of the laboratory direct shear test on the 60 by 60 mm rock joint sample tested by Johansson (2016) and the numerical direct shear tests in PFC^{2D} with profiles 1, 2 and 3 under a σ_n of 1 MPa

contact area more accurately. However, the computational time needed to conduct a numerical direct shear test in 3D would increase significantly.

A discrepancy was observed when comparing the post-peak ϕ simulated in PFC^{2D} to the residual behaviour measured in the actual rock joint tested in the laboratory. The simulated post-peak ϕ in the numerical shear tests on profiles 1, 2, and 3 after a δ_s of 1.5 mm was, on average, 31.7°. After the same δ_s, the measured post-peak ϕ in the rock joint tested in the laboratory was 52°. A possible reason for this discrepancy between the simulated and measured post-peak ϕ may be due to the fact that the SJCM installed in the numerical simulations performed in PFC^{2D} was set to small strain mode. This means that one particle in PFC^{2D} may have more than one active SJCM after the upper part of the numerical specimen has been sheared more than one particle diameter. This implies that the shear behaviour after large displacements (more than one particle diameter) may not be totally accurate. This may contribute to the observed discrepancy between the post-peak ϕ simulated in PFC^{2D} and that measured in the actual rock joint tested in the laboratory. Although the large strain mode can be

assigned to the installed SJCM, the validity of the results obtained by assigning this mode has not been proven in this study. Another possible reason for this discrepancy may be due to fewer contact points generated along the tested joint profiles in PFC^{2D} in comparison with the actual rock joint in 3D. Additionally, the upper part of the numerical specimen in PFC^{2D} was always sheared horizontally, and it was not able to tilt and accommodate during the numerical shear tests. This further contributes to fewer contact points compared with the actual shear test. This approach where the upper part is not able to tilt and accommodate has also been applied in previous research that uses PFC^{2D} to conduct numerical direct shear tests (Bahaaddini et al. 2013, 2014). A three-dimensional approach where the upper part of the sample can tilt and accommodate may therefore capture rock shear behaviour more accurately.

A second discrepancy was observed when comparing the δ_p in the numerical direct shear tests of the two-dimensional joint profiles in PFC^{2D} to that measured in the laboratory on the actual rock joint. The value of δ_p simulated in PFC^{2D} on the three joint profiles was, on average, 0.25 mm. The measured δ_p of the actual rock joint in the laboratory was 0.35 mm. The possible reason for this discrepancy between the simulated and measured δ_p may be due to the upper and lower parts of the actual rock joint having a small mismatch prior the laboratory test. This contributes to a less steep strength-displacement curve in the beginning of the shear test and a larger measured δ_p since this depends on

the shear stiffness of the asperities in contact during the shearing process (see Fig. 9). On the contrary, the upper and lower parts of the numerical specimens in PFC^{2D} had particle–particle contact along the joint profile before the direct shear tests were simulated. Furthermore, the slope of the strength-displacement curve in the numerical model in PFC^{2D} depends on both the shear and normal stiffness of the installed SJCM, and the stiffness of the PBM installed between the particles modelling the asperities. This discrepancy in the slope of the strength–displacement curve between shear tests performed in PFC^{2D} and in the laboratory has also been observed in previous studies (Li et al. 2020). This discrepancy may be reduced using a lower value of the shear stiffness of the SJCM assigned to the particles intersected by the simulated joint profile, to compensate for the high k_n value used to prevent particle interlocking derived using Eq. (1).

Influence of surface roughness resolution in the simulated shear strength in PFC^{2D}

To study the influence of the surface roughness resolution used in the joint profiles in PFC^{2D} on their simulated shear behaviour, a sensitivity analysis was performed on the SL and the P_{res}. Due to the relatively long computational time, this sensitivity analysis only included profile 3, which showed better agreement between the simulated ϕ_p in PFC^{2D} and that measured in the laboratory (see Fig. 9). This sensitivity analysis included four additional

numerical direct shear tests under a constant σ_n of 1 MPa. The micro-parameters of the PBM and the properties of the SJCM used in the numerical simulations are provided in Tables 2 and 3. Two tests were first performed in PFC^{2D} using values of SL of 0.6 and 1.2 mm, respectively. The value of R_{avg} was 0.08 mm, as in section "Numerical direct shear test in PFC^{2D} of an actual rock joint in granite". In these two numerical direct shear tests, the value of P_{res} increased from 2 to 3.4 and 6.9 particles, respectively. The results of ϕ versus δ_s for these two numerical shear tests are illustrated in Fig. 10a. The other two additional tests were performed with value of SL of 0.3 mm (i.e., as in section "Numerical direct shear test in PFC^{2D} of an actual rock joint in granite") and values of R_{avg} of 0.18 and 0.27 mm, respectively. The value of P_{res} in these numerical tests decreased from 2 to 0.75 and 0.5 particles, respectively. The results of ϕ versus δ_s for these two numerical shear tests are illustrated in Fig. 10b.

The results illustrated in Fig. 10a show that the simulated ϕ_p in PFC^{2D} with a R_{avg} of 0.08 mm and values of SL of 0.6 and 1.2 mm were 61.5° and 61.1°, respectively. The values of δ_p in the numerical simulations were 0.33 and 0.25 mm, respectively. These values of ϕ_p are lower than both the simulated ϕ_p and the measured ϕ_p of the actual rock joint (see Fig. 9). Furthermore, the numerical simulations in Fig. 10a had a larger δ_p and a smoother transition between peak and post-peak behaviour than the numerical simulation in Fig. 9. These results are not surprising, since part of the joint surface information captured in the measurements with optical
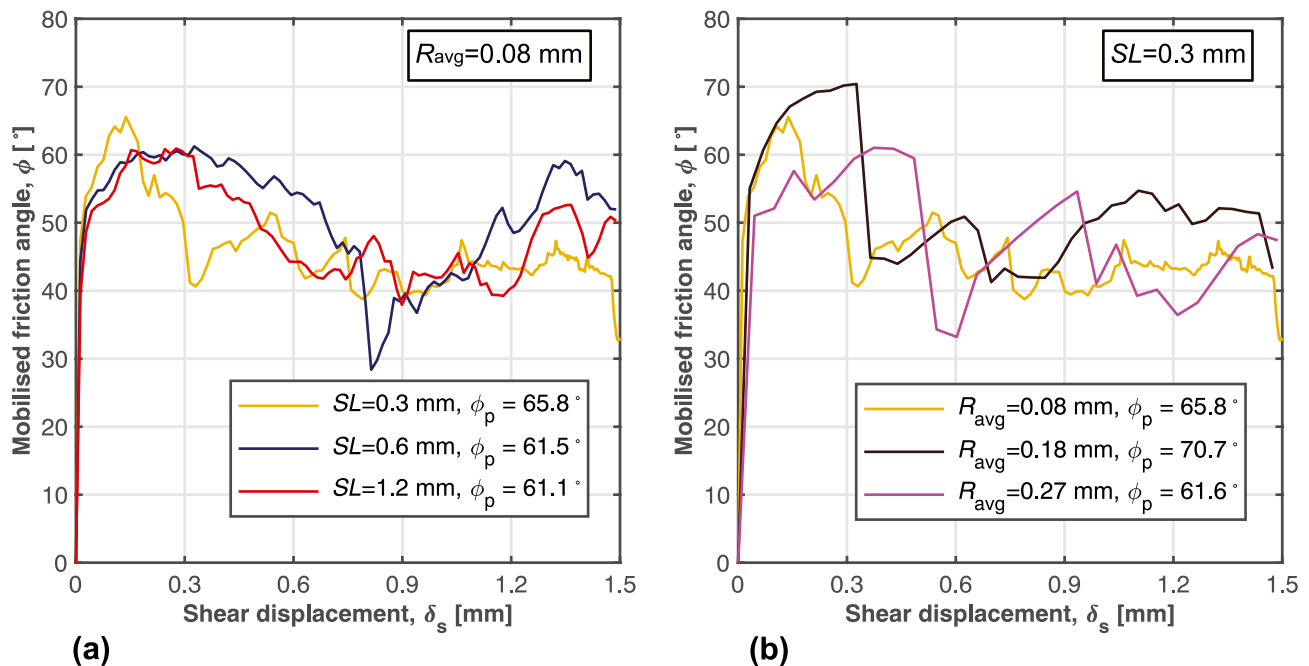
Fig. 10 Results of mobilised friction angle, ϕ vs. shear displacement, δ_s of profile 3 simulated in PFC^{2D} under a σ_n of 1 MPa: **a** with a R_{avg} of 0.08 mm and values of SL of 0.3, 0.6 and 1.2 mm; **b** with a SL of 0.3 mm and values of R_{avg} of 0.08, 0.18 and 0.27 mm

scanning is missed when SL values larger than the grain size are used in the numerical simulations. Therefore, the results presented in Fig. 10a show the importance of using a value of SL in PFC^{2D} that realistically captures the surface roughness of the actual rock joint at grain scale.

The results illustrated in Fig. 10b show that the simulated ϕ_p with a SL of 0.3 mm and values of R_{avg} of 0.18 and 0.27 mm were 70.7° and 61.6°, respectively. The values of δ_p in the numerical simulations were 0.32 and 0.4 mm, respectively. These values of ϕ_p are both higher and lower than the simulated ϕ_p shown in Fig. 9 using the same joint profile. The values of δ_p in the two numerical simulations in Fig. 10b were also larger than the δ_p obtained in Fig. 9 using the same joint profile. Furthermore, the match between the ϕ_p obtained in these two additional simulations in PFC^{2D} and the ϕ_p measured in the actual rock joint was not good. A possible reason for this mechanical behaviour observed in PFC^{2D} is that using a value of SL that captures surface roughness at grain scale but with an overly large particle size is incorrect. This means that filling the simulated SL in PFC^{2D} with sufficient P_{res} is necessary to achieve a good representation of the surface roughness of an actual rock joint at grain scale. The results obtained in the numerical simulation with profile 3 using a SL of 0.3 mm and a R_{avg} of 0.08 mm show that a P_{res} of at least 2 particles per joint segment captures the mechanical behaviour of the actual rock joint. Thus, using SL of 0.3 mm and a P_{res} of at least 2 particles per joint segment yields results in line with the

observations made in the laboratory by Johansson (2016) on the actual granite samples. Therefore, prior to numerical shear testing of perfectly mated rock joints using PFC^{2D}, it is recommended that a SL of 0.3 mm and a P_{res} of at least 2 particles per joint segment should be used.

Influence of the calibrated micro-properties and particle packing arrangement on the simulated shear strength in PFC^{2D}

To study the influence of the calibrated micro-properties of the PBM and the particle packing arrangement on the simulated shear strength in PFC^{2D}, a sensitivity analysis using profile 3 was performed. This sensitivity analysis included two additional series of numerical direct shear tests performed under a σ_n of 1 MPa using two different calibrated micro-properties of the PBM and five different values of S_{RN}. The values of SL and R_{avg} utilised were 0.3 and 0.08 mm, respectively (as in section "Numerical direct shear test in PFC^{2D} of an actual rock joint in granite"). The first series of numerical direct shear tests was performed using the micro-parameters of the PBM and properties of the installed SJCM provided in Tables 2 and 3. The results of ϕ versus δ_s for this series of numerical simulations using five different values of S_{RN} are illustrated in Fig. 11a. The numerical shear test with $S_{RN} = 10,001$ is the same as the one illustrated in Fig. 9.
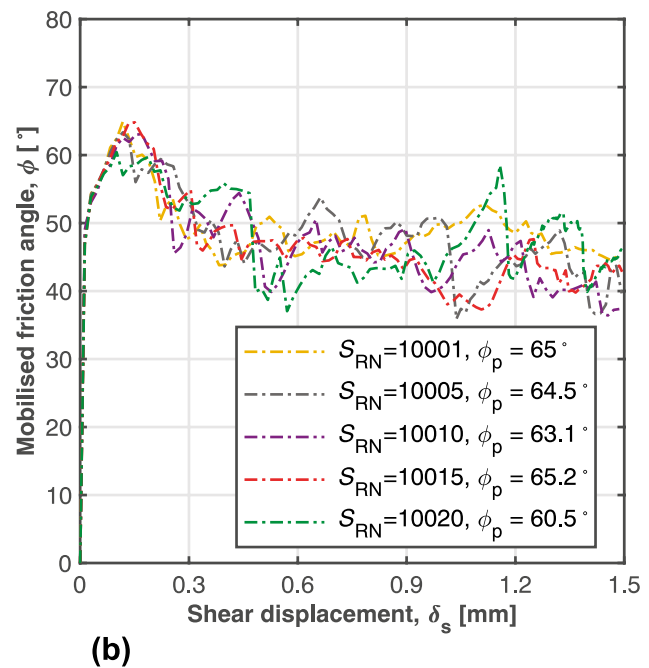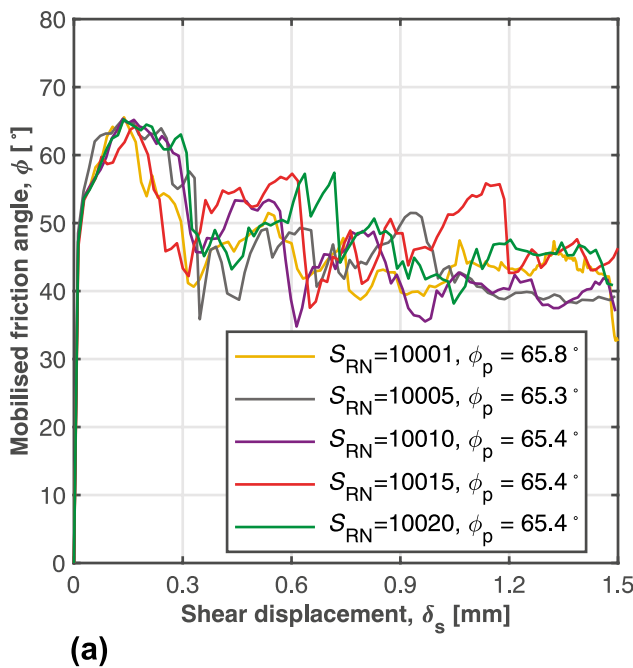
Fig. 11 Results of mobilised friction angle, ϕ vs. shear displacement, δ_s of profile 3 under a σ_n of 1 MPa and using five different values of S_{RN} in the specimen generation in PFC^{2D}: **a** with calibrated micro-properties of the PBM in the numerical UCS tests using a P_{res} of 6 particles; **b** with calibrated micro-properties of the PBM in the numerical UCS tests using a P_{res} of 20 particles

The second series of numerical direct shear tests was performed using different micro-properties of the PBM. A new intact rock calibration process following the steps described in section "Calibration of the intact rock and smooth-joint contact model parameters" was conducted. The main difference between the new calibration and that presented in section "Calibration of the intact rock and smooth-joint contact model parameters" is that the 50 by 100 mm numerical specimens were filled with particles having values of $R_{avg} = 1.15$ mm, $n_c = 0.08$, and $P_{res} = 20$ particles. Parallel bonds were installed at each particle–particle contact with an installation gap less than or equal to 30% of the R_{min} value. The average values of σ_{ci}, E_i, and ν_i simulated in the new calibration were 195.9 MPa, 84.4 GPa, and 0.26, respectively. These simulated values are in good agreement with the macro-properties measured for the intact granite rock in the laboratory (see Table 1). The simulated values of σ_{ci}, E_i and ν_i had a SD of 15.9 MPa, 1.42 GPa, and 0.006, respectively. This gave a COV of 8.1% for σ_{ci}, 1.7% for E_i and 2.3% for ν_i. The calibrated micro-properties of the PBM obtained with the new calibration are provided in Table 4. The results of ϕ versus δ_s using the micro-parameters of the PBM in Table 4, and the properties of the installed SJCM provided in Table 3 with five different values of S_{RN} are illustrated in Fig. 11b.

The results illustrated in Fig. 11a show that the series of numerical shear tests performed with the micro-properties in Table 2 had, on average, a simulated ϕ_p in PFC^{2D} of 65.5°. The difference between the average value of the simulated ϕ_p and that measured in the actual rock joint tested in the laboratory was 0.5°. The numerical shear tests with different S_{RN} had a SD of 0.2°. On the other hand, the results illustrated in Fig. 11b show that the series of numerical shear tests performed with the micro-properties in Table 4, which were lower than the micro-properties in Table 2, had, on average, a simulated ϕ_p in PFC^{2D} of 63.7°. Compared to the ϕ_p measured in the laboratory test, the average value of simulated ϕ_p in Fig. 11b was 1.3° lower. Furthermore, the SD in this second series of numerical shear tests was 1.9°.

The results illustrated Fig. 11a and b show that the average values of ϕ_p simulated with the micro-properties presented in Tables 2 and 4, respectively, and different values of S_{RN} are in good agreement with the measured ϕ_p of the actual rock joint. A possible reason for this observation is

that under low applied σ_n, the predominant failure mode governing the shearing process is sliding along the active asperities. This can be observed in Fig. 8, where only some parts of the tested profiles developed tensile cracks superficially. For this reason, under a σ_n of 1 MPa, the difference between ϕ_p simulated in PFC^{2D} using different micro-parameters of the PBM was not significantly large.

To increase the completeness of this sensitivity analysis, a third series of direct shear tests was performed in which the applied σ_n was increased to 5 and 10 MPa, respectively. The numerical specimens were generated using both the simulated micro-properties of the PBM in Tables 2 and 4, respectively. For simplicity, only two different values of S_{RN} were used. The values of ϕ_p simulated in PFC^{2D} were compared with the ϕ_p extrapolated for higher applied σ_n using the back-calculated value of JRC of the actual rock joint tested in the laboratory under a σ_n of 1 MPa (Barton and Choubey 1977). The value of JRC back-calculated based on the laboratory test of the actual rock joint was 14.9. The results of ϕ_p versus σ_n are illustrated in Fig. 12. The results show that under an applied σ_n of 5 and 10 MPa, the values of ϕ_p simulated in the numerical specimens using the micro-properties of the PBM in Table 4 were, on average, 2.1° and 3.8° lower than the extrapolated values of ϕ_p with a JRC of 14.9, respectively. Compared with the extrapolated values of ϕ_p using a JRC of 14.9, the values of ϕ_p simulated in the numerical specimens with micro-properties of the PBM in Table 2 were, on average, 1.0° and 1.2° lower, respectively. The values of ϕ_p simulated in the numerical specimens with micro-properties of the PBM in Table 2 were in better agreement with the extrapolated values ϕ_p for the actual rock joint. The reason for this is that the P_{res} during calibration of PBM micro-properties was 6 particles for properties in Table 2, and 20 particles for properties in Table 4, respectively. Thus, the micro-properties in Table 4 obtained with a P_{res} of 20 particles overestimate the number of particles that simulates the asperities in contact during the shearing process with profile 3, leading to an overall softer behaviour of the intact rock.

The results presented in this sensitivity analysis show the importance of understanding well how the number and size of the contact points generated in the joint profile during a numerical direct shear test in PFC^{2D} contribute to simulating the peak shear strength. Additionally, the results presented in Fig. 12 show that the shear test environment in

Table 4 Calibrated micro-properties of the PBM obtained in the numerical UCS tests in PFC^{2D} with a P_{res} of 20 particles per width of the numerical specimen

Particle properties		Parallel bond properties	
Particle density [kg/m^3]	2660	Young's modulus [GPa]	62.0
Young's modulus [GPa]	62.0	Cohesive strength [MPa]	97 ± 19.4
Friction coefficient [-]	2.5	Tensile strength [MPa]	97 ± 19.4
Normal to shear stiffness ratio [-]	5.0	Normal to shear stiffness ratio [-]	5.0
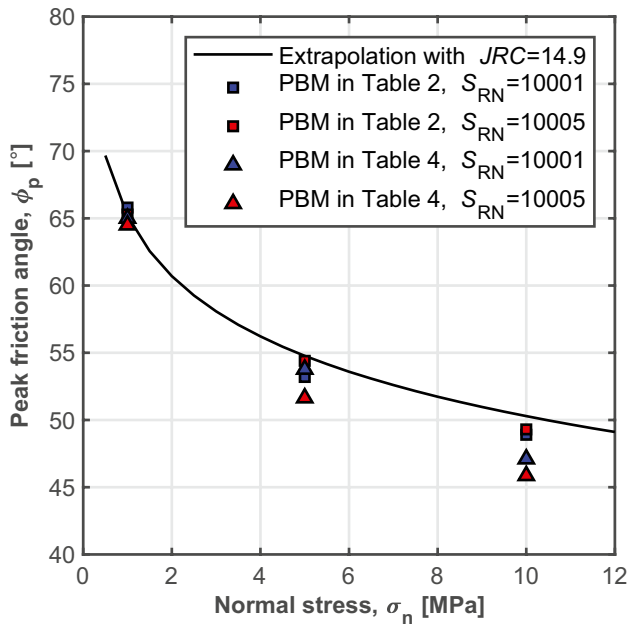
Fig. 12 Results of ϕ_p under different applied σ_n simulated in PFC^{2D} with profile 3 using two different values of S_{RN}, calibrated microproperties of the PBM with a P_{res} of 6 and 20 particles, respectively, and its comparison with the ϕ_p extrapolated by back-calculating the value of *JRC* of the actual rock joint, as proposed by Barton and Choubey (1977), based on the laboratory test with a σ_n of 1 MPa

PFC^{2D}, which has been validated against a laboratory shear test under a σ_n of 1 MPa, may be able to simulate the peak shear strength of actual rock joint profiles (2D) up to a σ_n of 10 MPa. However, it is possible that above this magnitude of σ_n, asperity breakage increases, and it may be necessary to use flat-jointed bonded-particle material to simulate the mechanical behaviour of the intact rock under such a high level of confinement (Potyondy 2018b). The main advantage of the flat-joint model is that it allows for the calibration of the bonded material against the compressive to tensile strength ration. This is an ability that parallel-bonded material lacks. However, the used of flat-jointed material requires also more computational power.

Conclusions

In this paper, we investigate the capability of PFC^{2D} to realistically simulate the shear strength of hard crystalline rock joints under different applied magnitudes of σ_n with surface roughness obtained from optical scanning measurements. Based on the simulations performed with two-dimensional profiles selected from the digitised rock joint surface, it can be concluded that the numerical shear test environment in PFC^{2D} presented in this paper has the capability of capturing the principal shear behaviour of actual rock joints under the conditions tested in this study.

The results of the simulations performed in the shear test environment in PFC^{2D} show that it is possible to match the peak shear strength of the actual rock joint of granite tested in the laboratory by selecting the two-dimensional profile in the shear direction that contains the steepest asperity. The results of the sensitivity analysis performed in PFC^{2D} show that to accurately capture the surface roughness of actual rock joints, a magnitude of joint segment length that captures grain size and at least two particles per segment are both needed. Additionally, the sensitivity analysis performed with different properties of the PBM shows that weaker bonds have a greater influence on the simulated peak shear strength with applied normal stresses higher than 10 MPa. This highlights the importance of adapting the calibration of the bond properties between particles in PFC^{2D} to simulate the size and failure mechanism of the active asperities in contact during the shearing process.

The post-peak shear strength obtained in the numerical simulations on the joint profiles was lower than that measured in the laboratory. The use of a small strain mode during the numerical simulations in the shear test environment in PFC^{2D} may have an influence on the simulated residual behaviour. Furthermore, the 2D approach together with the inability of the upper part of the samples to freely rotate in the PFC^{2D} environment generates fewer contact points compared to the 3D approach. In order to be able to realistically model the complete shear behaviour of rock joints in the future (i.e., including residual shear strength), a three-dimensional approach is recommended. In addition, the shear box should have the ability to let the upper part of the sample freely rotate in the same way as in actual shear tests. By doing so, a more accurate number and size for the contact points will be obtained.

The methodology in PFC^{2D} presented in this study has been tested to simulate the shear behaviour of an actual rock joint sample of granite to realistically account for its surface roughness and asperity strength. However, the segment length value required to accurately capture grain size may be different for other rock types. Both experimental work and numerical simulations are recommended to investigate the combination of scanning measurements and calibration of PFC parameters in order to simulate the shear behaviour of rock joints in other type of rocks. The practical implications of this methodology are that surface scanning measurements may be used to simulate the shear behaviour in 2D using the joint profile containing the steepest asperity. However, the presented methodology has only been used to simulate the shear behaviour of an actual rock joint sample with perfect match between its contact surfaces. Further studies are required to study the applicability of numerical techniques to simulate the shear behaviour of actual rock joints without perfect match between the contact surfaces.

Declarations

Competing interests The authors declare that they have no known competing financial interests or personal relationships that could have appeared to influence the work reported in this paper.

References

Asadi MS, Rasouli V, Barla G (2012) A bonded particle model simulation of shear strength and asperity degradation for rough rock fractures. Rock Mech Rock Eng 45:649–675. https://doi.org/10.1007/s00603-012-0231-4

Bahaaddini M, Hagan P, Mitra R, Hebblewhite B (2014) Scale effect on the shear behaviour of rock joints based on a numerical study. Eng Geol 181:212–223. https://doi.org/10.1016/j.enggeo.2014.07.018

Bahaaddini M, Sharrock G, Hebblewhite B (2013) Numerical direct shear tests to model the shear behaviour of rock joints. Comput Geotech 51:101–115. https://doi.org/10.1016/j.compgeo.2013.02.003

Ban L, Du W, Qi C (2020) A Peak Dilation Angle Model Considering the Real Contact Area for Rock Joints. Rock Mech Rock Eng 53:4909–4923. https://doi.org/10.1007/s00603-020-02193-1

Barton N, Choubey V (1977) The shear strength of rock joints in theory and practice. Rock Mech 10:1–54. https://doi.org/10.1007/BF01261801

Casagrande D, Buzzi O, Giacomini A, Lambert C, Fenton G (2018) A new stochastic approach to predict peak and residual shear strength of natural rock discontinuities. Rock Mech Rock Eng 51:69–99. https://doi.org/10.1007/s00603-017-1302-3

Castro-Filgueira U, Alejano LR, Mas Ivars D (2020) Particle flow code simulation of intact and fissured granitic rock samples. J Rock Mech Geotech Eng 12:960–974. https://doi.org/10.1016/j.jrmge.2020.01.005

Cundall PA (2000) Numerical experiments on rough joints in shear using a bonded particle model. In: Lehner FK, Urai JL (eds) Aspects of tectonic faulting. Springer, Berlin, Heidelberg, pp 1–9. https://doi.org/10.1007/978-3-642-59617-9_1

Grasselli G (2001) Shear strength of rock joints based on quantified surface description. EPFL Lausanne (Doctoral Thesis)

Grasselli G, Egger P (2003) Constitutive law for the shear strength of rock joints based on three-dimensional surface parameters. Int J Rock Mech Min Sci 40:25–40. https://doi.org/10.1016/S1365-1609(02)00101-6

Grasselli G, Wirth J, Egger P (2002) Quantitative three-dimensional description of a rough surface and parameter evolution with shearing. Int J Rock Mech Min Sci 39:789–800. https://doi.org/10.1016/S1365-1609(02)00070-9

Gutiérrez-Ch J, Senent S, Melentijevic S, Jimenez R (2018) Distinct element method simulations of rock-concrete interfaces under different boundary conditions. Eng Geol 240:123–139. https://doi.org/10.1016/j.enggeo.2018.04.017

Itasca Consulting Group (2018) PFC^{2D} Manual, version 5.0. Minneapolis, Minnesota

Johansson F (2016) Influence of scale and matedness on the peak shear strength of fresh, unweathered rock joints. Int J Rock Mech Min Sci 82:36–47. https://doi.org/10.1016/j.ijrmms.2015.11.010

Johansson F, Stille H (2014) A conceptual model for the peak shear strength of fresh and unweathered rock joints. Int J Rock Mech Min Sci 69:31–38. https://doi.org/10.1016/j.ijrmms.2014.03.005

Ladanyi B, Archambault G (1969) Simulation of shear behavior of a jointed rock mass. The 11th US Symposium on Rock Mechanics (USRMS). American Rock Mechanics Association

Lambert C, Coll C (2014) Discrete modeling of rock joints with a smooth-joint contact model. J Rock Mech Geotech Eng 6:1–12. https://doi.org/10.1016/j.jrmge.2013.12.003

Lazzari E, Johansson F, Mas Ivars D, Sánchez Juncal A (2014) Advances, Current Limitations and Future Requirements for a Numerical Shear Box for Rock Joints Using PFC 2D. ISRM Regional Symposium-EUROCK 2014. International Society for Rock Mechanics and Rock Engineering

Li H, Deng J, Yin J, Zhu J (2020) Modelling the shearing behaviour of joints using an improved shear box genesis approach in particle flow code (2D) and its validation. Geomech Geophys Geo-Energ Geo-Resour 6:1–15. https://doi.org/10.1007/s40948-019-00138-9

Mas Ivars D, Pierce ME, Darcel C, Reyes-Montes J, Potyondy DO, Young RP, Cundall PA (2011) The synthetic rock mass approach for jointed rock mass modelling. Int J Rock Mech Min Sci 48:219–244. https://doi.org/10.1016/j.ijrmms.2010.11.014

Mas Ivars D, Potyondy D, Pierce M, Cundall P (2008) The Smooth-Joint Contact Model. 8th World Congress on Computational Mechanics and 5th European Congress on Computational Methods in Applied Sciences and Engineering. Venice, Italy

Mehranpour MH, Kulatilake PH (2017) Improvements for the smooth joint contact model of the particle flow code and its applications. Comput Geotech 87:163–177. https://doi.org/10.1016/j.compgeo.2017.02.012

Park J-W, Song J-J (2009) Numerical simulation of a direct shear test on a rock joint using a bonded-particle model. Int J Rock Mech Min Sci 46:1315–1328. https://doi.org/10.1016/j.ijrmms.2009.03.007

Patton FD (1966) Multiple modes of shear failure in rock. 1st ISRM Congress. International Society for Rock Mechanics

Potyondy D (2018a) Material-Modeling Support in PFC [fistPkg26]. Technical Memorandum ICG7766-L. Minneapolis, Minnesota

Potyondy D (2018b) A Flat-Jointed Bonded-Particle Model for Rock. 52nd US Rock Mechanics/Geomechanics Symposium, Seattle, Washington. American Rock Mechanics Association

Potyondy DO, Cundall P (2004) A bonded-particle model for rock. Int J Rock Mech Min Sci 41:1329–1364. https://doi.org/10.1016/j.ijrmms.2004.09.011

Ríos-Bayona F, Johansson F, Larsson J, Mas-Ivars D (2022) Peak Shear Strength of Natural, Unfilled Rock Joints in the Field Based on Data from Drill Cores – A Conceptual Study Based on Large

Laboratory Shear Tests. Rock Mech Rock Eng. https://doi.org/10.1007/s00603-022-02913-9

Ríos-Bayona F, Johansson F, Mas-Ivars D (2021) Prediction of peak shear strength of natural, unfilled rock joints accounting for matedness based on measured aperture. Rock Mech Rock Eng 54:1533–1550. https://doi.org/10.1007/s00603-020-02340-8

Ríos-Bayona F, Stigsson M, Johansson F, Mas Ivars D (2018) Comparison between shear strength based on Barton's roughness profiles and equivalent synthetic profiles based on fractal theory. 52nd US Rock Mechanics/Geomechanics Symposium, Seattle, Washington. American Rock Mechanics Association

Sinha S, Walton G (2020) A study on Bonded Block Model (BBM) complexity for simulation of laboratory-scale stress-strain behavior in granitic rocks. Comput Geotech 118:103363. https://doi.org/10.1016/j.compgeo.2019.103363

Tang J-Z, Yang S-Q, Elsworth D, Tao Y (2020) Three-Dimensional Numerical Modeling of Grain-Scale Mechanical Behavior of Sandstone Containing an Inclined Rough Joint. Rock Mech Rock Eng 54:905–919. https://doi.org/10.1007/s00603-020-02281-2

Tatone BS, Grasselli G (2009) A method to evaluate the three-dimensional roughness of fracture surfaces in brittle geomaterials. Rev Sci Instrum 80:125110. https://doi.org/10.1063/1.3266964

Yang J, Rong G, Hou D, Peng J, Zhou C (2016) Experimental study on peak shear strength criterion for rock joints. Rock Mech Rock Eng 49:821–835. https://doi.org/10.1007/s00603-015-0791-1